

# Radiative Corrections in Bound States: Recent Results

---

**Andrzej Czarnecki<sup>a,\*</sup> and Artem O. Davydov<sup>a</sup>**

<sup>a</sup>*Department of Physics, University of Alberta,  
T6G 2G7, Edmonton, Canada*

*E-mail:* [andrzejc@ualberta.ca](mailto:andrzejc@ualberta.ca), [davydov@ualberta.ca](mailto:davydov@ualberta.ca)

Two recent studies of radiative corrections to bound state properties are discussed. The change of the decay rate of a muon bound to a light nucleus has been calculated for several light nuclei  $4 \leq Z \leq 9$  with high precision, resolving a long-standing discrepancy between analytical and numerical results for oxygen ( $Z = 8$ ). The decay of parapositronium into three photons has been calculated including effects of the  $Z$  boson. The resulting rate is many orders of magnitude smaller than previously estimated.

*Loops and Legs in Quantum Field Theory (LL2026)*  
*12–17 April, 2026*  
*Bayreuth, Germany*

---

\*Speaker

## 1. Introduction

The muon is similar to the electron in most respects: both are leptons, carry identical electric charge, and have the same spin. However, the muon is approximately 207 times heavier than the electron. As a result of energy-momentum conservation, the muon can decay into an electron, while the electron is stable. The decay rate of a free muon is given by

$$\Gamma_0 = \frac{G_F^2 m_\mu^5}{192\pi^3}, \quad (1)$$

where  $m_\mu \approx 105.65$  MeV is the muon mass and  $G_F$  is the Fermi constant. In the present discussion we focus on the ratio of the decay rate  $\Gamma$  of a muon bound to a light nucleus to  $\Gamma_0$  of a free muon. Muonic atoms offer probes of physics beyond the Standard Model [1, 2], especially for searches for the charged-lepton-flavor-violating (CLFV) coherent muon-to-electron conversion,  $\mu^- N \rightarrow e^- N$  [3–6]. For those experiments, the ordinary muon decay  $\mu^- N \rightarrow e^- N + \bar{\nu}_e + \nu_\mu$ , which does not violate lepton number conservation, is an irreducible background.

For the muon decay in orbit (DIO), an analytical perturbative calculation accurate to order  $(\alpha Z)^2$  was carried out in Ref. [7]:

$$\Gamma/\Gamma_0 = f(x_e) \left( 1 - \frac{(\alpha Z)^2}{2} \right) + \mathcal{O}((\alpha Z)^3), \quad (2)$$

where  $f(x_e)$  accounts for the finite electron mass,

$$f(x_e) = 1 - 8x_e^2 - 24x_e^4 \ln x_e + 8x_e^6 - x_e^8 = 0.99981, \quad x_e \equiv \frac{m_e}{m_\mu} = 4.8363 \times 10^{-3}. \quad (3)$$

However, a fully relativistic calculation of the total DIO rate based on a partial-wave expansion [8] showed a significant deviation from this prediction for oxygen ( $Z = 8$ ). The numerical result reported in Ref. [8] is  $\Gamma/\Gamma_0 = 0.994$ , while formula (2) gives  $\Gamma/\Gamma_0 = 0.9981$ . The expected next-to-leading  $(\alpha Z)^3$  correction,  $(\alpha Z)^3 \sim 2 \times 10^{-4}$ , is more than an order of magnitude smaller than the observed discrepancy and cannot explain it. In [9] we reexamined the DIO rate for oxygen and showed that the discrepancy originated from too early truncation of a slowly convergent partial-wave series. To support this conclusion, we also calculated the decay rate for other nuclei in the range  $4 \leq Z \leq 9$  and showed that the deviation between our all-order-in- $\alpha Z$  numerical results and the analytical expression (2) decreases smoothly as  $Z \rightarrow 0$ , confirming that the difference is accounted for by higher-order corrections  $\mathcal{O}((\alpha Z)^3)$ .

Below we describe that work, and then a second bound-state decay where explicit calculation likewise corrects an earlier estimate: parapositronium into three photons. It is forbidden in pure QED but opened by the C-violating weak interaction. Its rate proves orders of magnitude below the original guess.

## 2. Theoretical framework

Following Refs. [10, 11], we factorize the bound decay into the cascade  $(Z\mu^-) \rightarrow [Ze^-]A$  and  $A \rightarrow \bar{\nu}_e \nu_\mu$ , with  $A$  a fictitious massive neutral vector carrying the flavor of the neutrino pair.

Here  $(Z\mu^-)$  is a muon bound in the nuclear field and  $[Ze^-]$  a continuum electron in that field. The decay rate reads

$$\Gamma((Z\mu^-) \rightarrow [Ze^-] \bar{\nu}_e \nu_\mu) = \frac{256\pi \Gamma_0}{g^2 m_\mu} \int_0^{z_{\max}} dz \Gamma((Z\mu^-) \rightarrow [Ze^-] A) z^3, \quad (4)$$

where the dimensionless variable  $z$  is defined as

$$z \equiv \frac{m_A}{m_\mu}, \quad 0 \leq z \leq z_{\max} = \frac{E_\mu - E_e}{m_\mu}, \quad (5)$$

and  $g$  is the weak-coupling constant,  $m_A$  is the invariant mass of the intermediate boson  $A$ , with  $E_\mu$  and  $E_e$  being the total energies of the initial-state muon and the final-state electron, respectively.

The two-body decay rate  $\Gamma((Z\mu^-) \rightarrow [Ze^-] A)$  is given by

$$\Gamma((Z\mu^-) \rightarrow [Ze^-] A) = \frac{1}{64\pi^5} \int \frac{d^3 \vec{p}_e}{p_e E_e} \frac{d^3 \vec{k}}{k_0} \delta(E_\mu - E_e - k_0) |\mathcal{M}_{(Z\mu^-) \rightarrow [Ze^-] A}|^2, \quad (6)$$

where  $p_e^\nu = (E_e, \vec{p}_e)$  with  $p_e \equiv |\vec{p}_e|$  and  $k^\nu = (k_0, \vec{k})$  are the four-momenta of the outgoing electron and the intermediate boson  $A$ , respectively. The squared amplitude reads

$$|\mathcal{M}_{(Z\mu^-) \rightarrow [Ze^-] A}|^2 = \frac{1}{2} \sum_{\mu_\mu} \sum_{\kappa_e \mu_e} \frac{g^2}{2} J^\alpha(\vec{k}) J^{\dagger\beta}(\vec{k}) \left( -g_{\alpha\beta} + \frac{k_\alpha k_\beta}{m_A^2} \right), \quad (7)$$

where the leptonic currents  $J^\alpha(\vec{k})$  are overlap integrals between the muon wave function  $\Psi_{\mu_\mu}(\vec{r})$  and the electron wave function  $\psi_{E_e \kappa_e \mu_e}(\vec{r})$ :

$$J_\alpha(\vec{q}) = \int d^3 \vec{r} e^{-i\vec{q}\cdot\vec{r}} \psi_{E_e \kappa_e \mu_e}^\dagger(\vec{r}) \gamma_0 \gamma_\alpha P_L \Psi_{\mu_\mu}(\vec{r}). \quad (8)$$

The angular integrations in (8) and (7), as well as the summations over the total angular momentum projections  $\mu_\mu$  and  $\mu_e$ , can be performed analytically [8, 12–14], leading to the following representation of the decay rate:

$$\frac{\Gamma}{\Gamma_0} = \sum_{\kappa_e} \frac{\Gamma_{\kappa_e}}{\Gamma_0}, \quad (9)$$

where  $\Gamma_{\kappa_e}$  are the partial-wave contributions evaluated numerically.

### 3. Numerical results and discussion

We evaluate  $\Gamma/\Gamma_0$  from Eqs. (4)–(9) for point-Coulomb nuclei,  $4 \leq Z \leq 9$ . The muon enters through the closed-form Dirac–Coulomb ground state [15]; the continuum electron comes from integrating the Dirac equation with RADIAL [16, 17] in double-precision. The radial integrals oscillate strongly and are handled with the adaptive DQAGS routine of QUADPACK [18] at  $10^{-9}$  tolerance. We extend the  $\kappa_e$  sum until term-to-term changes reach  $10^{-5}$ – $10^{-6}$  and fix the tail with a geometric estimate.

In Table 1 we present the converged results for  $\Gamma/\Gamma_0$  and compare them with Refs. [7, 8, 19]. In Ref. [19] the charge distribution based on modern experimental data was taken into account and the

**Table 1:** The total bound-muon decay rate normalized to the free-muon rate,  $\Gamma/\Gamma_0$ , for various atomic numbers  $Z$ . The second and third columns show results of the fully relativistic calculation of the present work (PW) and Ref. [8], respectively. The fourth column shows results from the perturbative  $\alpha Z$  expansion of Ref. [7] corrected for the finite electron mass. The fifth column shows isotope-averaged results from Ref. [19]. The sixth column,  $\Delta(Z)$ , shows the difference between the  $\alpha Z$  results and the present work in units of  $10^{-3}$ .

$Z$	PW	Ref. [8]	Ref. [7]	Ref. [19]	$\Delta(Z) [10^{-3}]$
4	0.9993		0.9994		0.045
5	0.9990		0.9991		0.099
6	0.9987		0.9989	0.9987	0.188
7	0.9982		0.9985	0.9982	0.322
8	0.9976	0.994	0.9981	0.9977	0.506
9	0.9969		0.9977	0.9970	0.757

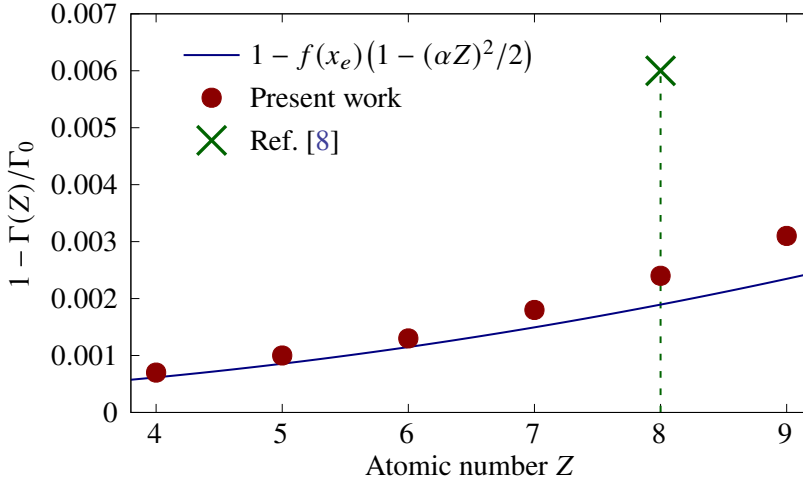


**Figure 1:** The quantity  $1 - \Gamma/\Gamma_0$  as a function of  $Z$ . Red circles: present work. Blue solid line: analytical approximation  $1 - f(x_e)(1 - (\alpha Z)^2/2)$ , where  $f(x_e)$  accounts for the finite electron mass. Green cross: result of Ref. [8] for  $Z = 8$ . The systematic excess of the red circles above the solid line reflects higher-order corrections in  $\alpha Z$ .

decay rates were averaged over different isotopes of each element. The agreement between Ref. [19] and our results confirms that the effect of the finite nuclear charge distribution is negligible for light nuclei.

Our results are visualized in Fig. 1, which plots  $1 - \Gamma/\Gamma_0$  versus  $Z$ . The solid line represents the  $(\alpha Z)^2$  prediction  $1 - f(x_e)(1 - (\alpha Z)^2/2)$  of Ref. [7], while the red circles denote the present all-order-in- $\alpha Z$  values. Our results lie consistently above the  $(\alpha Z)^2$  curve, and the magnitude of this excess grows with  $Z$ , as quantified by the positive  $\Delta(Z)$  values in Table 1. This trend is consistent with a negative next-order correction to  $\Gamma/\Gamma_0$  in the  $\alpha Z$  expansion. In contrast, the result of Ref. [8] for  $Z = 8$  (green cross in Fig. 1) deviates significantly from both our data and the  $(\alpha Z)^2$  prediction.

The origin of the discrepancy is revealed by Table 2, which contains the partial sums  $\sum_{|\kappa_e| \leq \kappa_{\max}} \Gamma_{\kappa_e}/\Gamma_0$  for different truncation limits  $\kappa_{\max}$ . The series converges slowly: even at  $\kappa_{\max} = 29$

the result  $\Gamma/\Gamma_0 = 0.99389$  is still far from the converged value. Ref. [8] terminated the expansion at  $L = 31$ , obtaining  $\Gamma/\Gamma_0 = 0.994$ , in good agreement with our unconverged partial sum at comparable  $\kappa_{\max} = 29$ . Only by extending the summation up to  $\kappa_{\max} = 59$  and extrapolating the remaining tail allowed us to obtain the converged result  $\Gamma/\Gamma_0 = 0.99760$ , which is consistent with the analytical prediction (2).

**Table 2:** Convergence of the partial-wave expansion for  $^{16}\text{O}$  ( $Z = 8$ ). Shown are the partial sums  $\sum_{|\kappa_e| \leq \kappa_{\max}} \Gamma_{\kappa_e}/\Gamma_0$  as a function of the cutoff  $\kappa_{\max}$ .

$\kappa_{\max}$	Present work	Ref. [8]
25	0.98871	
29	0.99389	0.994
35	0.99661	
40	0.99728	
45	0.99750	
50	0.99757	
55	0.99759	
59	0.99760	

#### 4. Decay of parapositronium into three photons

Positronium, with two spin-1/2 components: an electron and a positron, has a spin-0 ground state called parapositronium (pPs) and a spin-1 slightly excited state called orthopositronium (oPs). By the Landau-Yang theorem, oPs cannot decay into two photons, because of Bose-Einstein statistics and angular momentum conservation. A decay of oPs results in at least three photons. On the other hand, pPs does decay into two photons; can it decay also into three? The role of symmetries in the decays of positronium and related systems such as the  $\text{Ps}^-$  ion has very recently been discussed in [20], where further references can be found (see also [21]).

It turns out that in pure quantum electrodynamics (QED) pPs decays only into even numbers of photons because of charge-conjugation symmetry  $C$ . However, weak interactions violate  $C$  and enable the decay  $\text{pPs} \rightarrow 3\gamma$ . The rate of this decay was first estimated in [22]. Ref. [23] calculated the contribution of  $W$  loops to this channel. More recently, the full one-loop amplitude, including  $Z$ -boson contributions, has been determined [24].

These explicit calculations showed that the rate of  $\text{pPs} \rightarrow 3\gamma$  is smaller by many orders of magnitude than first estimated. One reason for this suppression is the vanishing of some classes of diagrams [24]. Here we illustrate that vanishing with the example of pPs annihilation that produces only a virtual  $Z$  boson, which then decays into three photons through a  $W$ -loop, as shown in Fig. 2.

A  $Z$  boson can decay into  $3\gamma$  [25]. That it cannot mediate  $\text{pPs} \rightarrow 3\gamma$  is best seen in the unitary gauge. Consider first the amplitude of annihilation  $\text{pPs} \rightarrow Z^*$ . Since pPs has no spin and  $Z$  has spin 1, that amplitude transforms as a Lorentz vector under rotations and boosts, so it must be proportional to  $q$ , the 4-momentum of pPs, the only 4-vector relevant for this process. The structure of the total amplitude is

$$\mathcal{M}(\text{pPs} \rightarrow Z^* \rightarrow 3\gamma) \propto q^\mu D_{\mu\nu}^Z \mathcal{M}^\nu(Z^* \rightarrow 3\gamma), \quad (10)$$

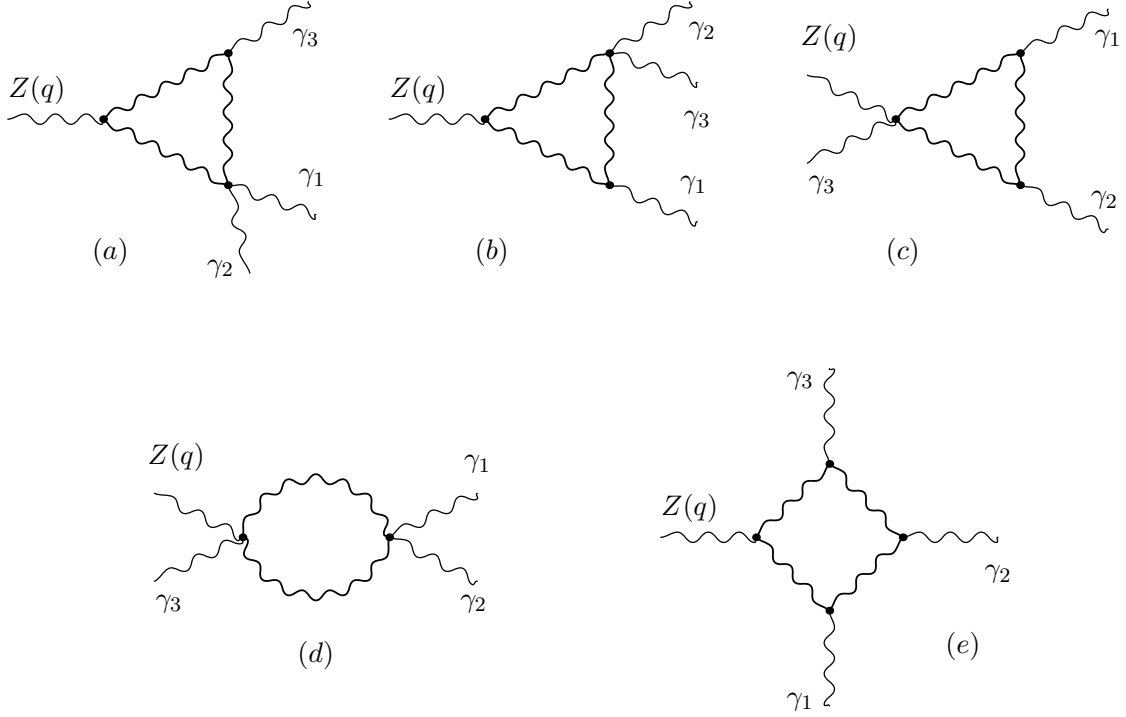


**Figure 2:** Representative  $W$ -loop diagrams contributing to  $Z^*(q) \rightarrow \gamma(k_1)\gamma(k_2)\gamma(k_3)$ . Diagrams (a) and (b) contain one AWW and one AAWW photon vertex, (c) contains one ZAWW and two AWW vertices, (d) contains one ZAWW and one AAWW vertex, and (e) contains three AWW vertices. The photon permutations are generated by  $S_3$ .

where we denote by  $D_{\mu\nu}^a$ , propagators of vector bosons,  $a = W, Z$ . In the unitary gauge we use

$$D_{\alpha\beta}^a(p) = \frac{i}{M_a^2 - p^2} \left( g_{\alpha\beta} - \frac{p_\alpha p_\beta}{M_a^2} \right), \quad D_{\alpha\beta}^{-1}(p) = i \left[ (p^2 - M_a^2) g_{\alpha\beta} - p_\alpha p_\beta \right], \quad a = W, Z. \quad (11)$$

The amplitude in Eq. (10) becomes

$$\mathcal{M}(\text{pPs} \rightarrow Z^* \rightarrow 3\gamma) \propto q_\nu \mathcal{M}^\nu(Z^* \rightarrow 3\gamma). \quad (12)$$

Below we show the vanishing of this contraction of the amplitude  $\mathcal{M}^\nu(Z^* \rightarrow 3\gamma)$  with the incoming momentum  $q$  of the  $Z$ -boson.

With all momenta at a vertex taken as incoming, define

$$\Gamma_{\alpha\beta\mu}(p_-, p_+, r) = (p_- - p_+)_\mu g_{\alpha\beta} + (p_+ - r)_\alpha g_{\beta\mu} + (r - p_-)_\beta g_{\mu\alpha}, \quad (13)$$

$$T_{\alpha\beta\mu\nu} = 2g_{\alpha\beta} g_{\mu\nu} - g_{\alpha\mu} g_{\beta\nu} - g_{\alpha\nu} g_{\beta\mu}. \quad (14)$$

Writing  $g_Z = ec_W/s_W$ , the required Feynman rules [26] are (we use  $e > 0$ )

$$V_{\alpha\beta\mu}^A = ie \Gamma_{\alpha\beta\mu}, \quad V_{\alpha\beta\mu}^Z = ig_Z \Gamma_{\alpha\beta\mu}, \quad (15)$$

$$V_{\alpha\beta\mu\nu}^{AA} = -ie^2 T_{\alpha\beta\mu\nu}, \quad V_{\alpha\beta\rho\mu}^{ZA} = -ie g_Z T_{\alpha\beta\rho\mu}. \quad (16)$$

The diagrammatic conventions corresponding to Eqs. (11), (15), and (16) are shown in Fig. 3.

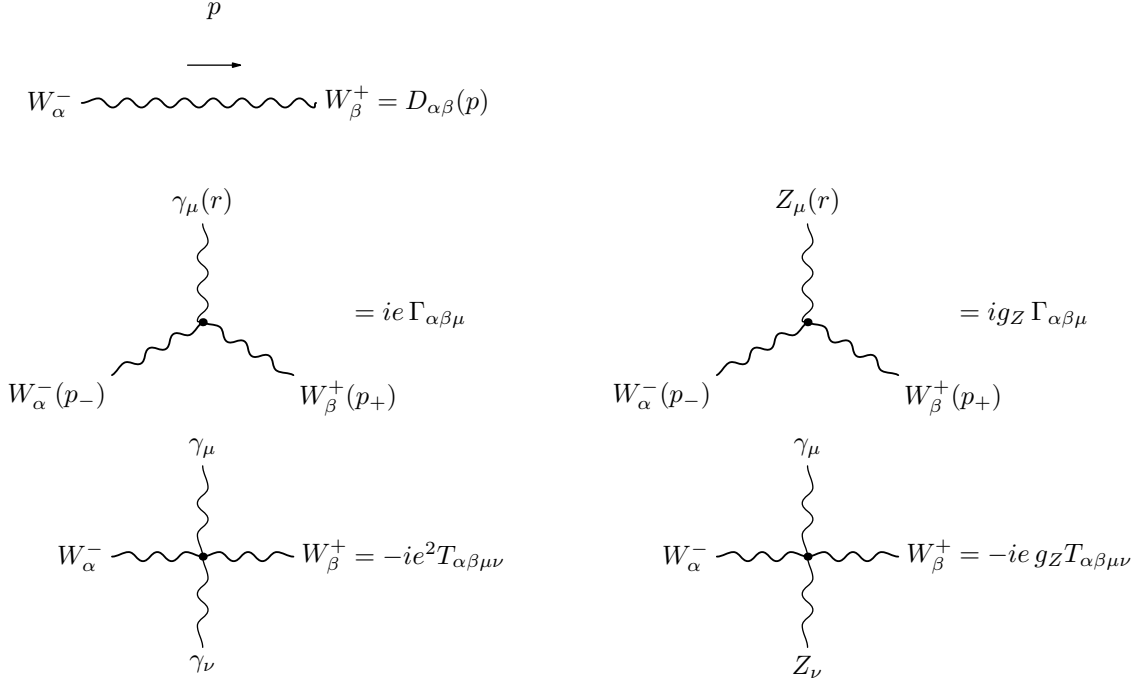


**Figure 3:** Unitary-gauge propagator and vertices used in the calculation. All momenta entering the vertex expressions are taken as incoming.

The elementary Ward identities following from Eqs. (15) and (16) are

$$q^\rho V_{\alpha\beta\rho}^Z(p_-, p_+, q) = g_Z \left[ D_{\alpha\beta}^{-1}(p_+) - D_{\alpha\beta}^{-1}(p_-) \right], \quad (17)$$

$$q^\rho V_{\alpha\beta\rho\mu}^{ZA}(p_-, p_+, q, k) = g_Z \left[ V_{\alpha\beta\mu}^A(p_-, p_+ + q, k) - V_{\alpha\beta\mu}^A(p_- + q, p_+, k) \right]. \quad (18)$$

Placing Eq. (17) between the two adjacent propagators and using Eq. (11) gives

$$D(p_-) q^\rho V_{\rho}^Z D(p_+) = g_Z [D(p_-) - D(p_+)]. \quad (19)$$

Thus contraction of a  $ZWW$  vertex removes either adjacent propagator, whereas contraction of a  $ZAWW$  vertex gives the difference of two  $AWW$  insertions, as displayed in Eq. (18).

The five representative topologies are shown in Fig. 2. After summing over the six permutations of the photons, denoted by  $\mathcal{S}_3$ , the amplitude is organized as

$$\mathcal{M}^\nu = \mathcal{S}_3 \left[ \frac{1}{2} (\mathcal{M}_a + \mathcal{M}_b + \mathcal{M}_d) + \mathcal{M}_c + \mathcal{M}_e \right]^\nu. \quad (20)$$

The factor  $1/2$  removes the double counting caused by interchanging the two photons attached to an  $AWW$  vertex.

The two terms in Eq. (20) are separately transverse. To see this, first remove the  $Z$  insertion. The diagrams (a), (b), and (d) arise from the same electromagnetic skeleton: a closed  $W$  loop with one  $AWW$  vertex and one  $AAWW$  vertex. Inserting the  $Z$  on either of its two  $W$  propagators gives (a) and (b), while replacing its  $AWW$  vertex by a  $ZAWW$  vertex gives (d). Equations (18)

and (19) turn the contraction with  $q$  into finite differences between neighboring insertions. These differences telescope around the closed loop, so

$$q_\nu \mathcal{S}_3 (\mathcal{M}_a + \mathcal{M}_b + \mathcal{M}_d)^\nu = 0. \quad (21)$$

The diagrams (c) and (e) arise from a second skeleton, containing three AWW vertices. Inserting the Z on its three W propagators produces the box diagrams (c), while replacing any AWW vertex by a ZAWW vertex produces the triangle diagrams (e). The same telescopic cancellation gives

$$q_\nu \mathcal{S}_3 (\mathcal{M}_c + \mathcal{M}_e)^\nu = 0. \quad (22)$$

The two sectors do not mix because contraction of the Z leg preserves the number of AAWW vertices. Equations (21) and (22) therefore prove the vanishing of the complete amplitude in Eq. (10).

## 5. Conclusion

We have reviewed the fully relativistic calculation of the bound-muon decay rate for light nuclei ( $4 \leq Z \leq 9$ ) that resolved the long-standing discrepancy between the all-order-in- $\alpha Z$  numerical approach and the perturbative analytical result of Ref. [7]. The discrepancy was traced to a premature truncation of the slowly convergent partial-wave series in Ref. [8]. Comparison with Ref. [19] confirms that finite nuclear charge distribution effects are negligible for the light nuclei considered here.

We have also reviewed a calculation of Z-boson contributions to the C-violating parapositronium decay into three photons. An early estimate of its rate turned out to be much too large because some diagrams are suppressed by small ratios of masses and some vanish exactly. We provided an example of a vanishing contribution and explained in some detail why it does not contribute.

## Acknowledgments

AC thanks Ting Gao for discussions of the amplitude of  $pPs \rightarrow 3\gamma$  and of reasons why some classes of diagrams do not contribute. This work was supported by the Natural Sciences and Engineering Research Council of Canada (NSERC).

## References

- [1] Y. Uesaka, M. Yamanaka, and Y. Kuno,  $\mu^- \rightarrow e^- \gamma$  in a muonic atom as a probe for effective lepton flavor-violating operators involving photon fields, *Phys. Rev. D* **111**, 035017 (2025), arXiv:2411.10304.
- [2] J. E. J. Matias, A. S. Lemos, and F. Dahia, *Probing Short-Distance Modifications of Gravity via Spin-Independent and Spin-Dependent Effects in Muonic Atoms* (2025), arxiv:2511.00719.
- [3] S. Miscetti, *Status of the Mu2e experiment*, *Nucl. Instrum. Meth. A* **1073**, 170257 (2025).

- [4] M. Aoki et al., *Charged Lepton Flavour Violations searches with muons: present and future* (2025), arxiv:2503.22461.
- [5] H. Nishiguchi, *A search for muon-to-electron conversion at J-PARC : The COMET experiment*, PoS **ICHEP2024**, 469 (2025).
- [6] K. Yamamoto, *DeeMe – Muon-Electron Conversion Search Experiment*, Phys. Sci. Forum **8**, 39 (2023).
- [7] H. Überall, *Decay of  $\mu^-$  Mesons Bound in the K Shell of Light Nuclei*, Phys. Rev. **119**, 365–376 (1960).
- [8] R. Watanabe, K. Muto, T. Oda, T. Niwa, H. Ohtsubo, R. Morita, and M. Morita, *Asymmetry and energy spectrum of electrons in bound-muon decay*, Atomic Data and Nucl. Data Tables **54**, 165 (1993).
- [9] A. Czarnecki, A. O. Davydov, and M. Y. Kaygorodov, *Total decay rate of a muon bound to a light nucleus*, Phys. Rev. D **113**, 036028 (2026), [2512.23023](#).
- [10] V. Gilinsky and J. Mathews, *Decay of bound muons*, Phys. Rev. **120**, 1450 (1960).
- [11] M. J. Aslam, A. Czarnecki, G. Zhang, and A. Morozova, *Decay of a bound muon into a bound electron*, Phys. Rev. D **102**, 073001 (2020), [2005.07276](#).
- [12] A. Czarnecki, X. Garcia i Tormo, and W. J. Marciano, *Muon decay in orbit: spectrum of high-energy electrons*, Phys. Rev. **D84**, 013006 (2011), [1106.4756](#).
- [13] R. Watanabe, M. Fukui, H. Ohtsubo, and M. Morita, *Angular distribution of electrons in bound muon decay*, Prog. Theor. Phys. **78**, 114 (1987).
- [14] M. Y. Kaygorodov, Y. S. Kozhedub, A. V. Malyshev, A. O. Davydov, Y. Wu, and S. B. Zhang, *Study of atomic effects on electron spectrum in bound-muon decay process*, Chin. Phys. C **50**, 063103 (2026), [2506.02416](#).
- [15] M. E. Rose, *Relativistic Electron Theory*, John Wiley, New York (1961).
- [16] F. Salvat, J. M. Fernández-Varea, and W. Williamson Jr, *Accurate numerical solution of the radial Schrödinger and Dirac wave equations*, Computer Physics Communications **90**, 151–168 (1995).
- [17] F. Salvat and J. M. Fernández-Varea, *RADIAL: A Fortran subroutine package for the solution of the radial Schrödinger and Dirac wave equations*, Computer Physics Communications **240**, 165–177 (2019).
- [18] R. Piessens, E. de Doncker-Kapenga, C. W. Überhuber, and D. K. Kahaner, *QUADPACK: a subroutine package for automatic integration*, Springer, Berlin (2012).
- [19] Y. Uesaka, T. Naito, S. Ebata, and M. Niikura, *Comprehensive table of calculated Huff factors*, Atomic Data and Nuclear Data Tables page 101809 (2026), arXiv:2602.07501.

- [20] N. U. Sani, M. J. Aslam, and I. Ahmed, *Weak decay of the positronium ion* (2026), arXiv:2606.25433.
- [21] S. D. Bass, *QED and Fundamental Symmetries in Positronium Decays*, Acta Phys. Polon. B **50**, 1319 (2019), [1902.01355](#).
- [22] W. Bernreuther and O. Nachtmann, *Weak Interaction Effects in Positronium*, Z. Phys. **C11**, 235 (1981).
- [23] A. Pokraka and A. Czarnecki, *Parapositronium can decay into three photons*, Phys. Rev. **D96**, 093002 (2017), [1707.09466](#).
- [24] A. Czarnecki, D. Dagia, T. Gao, and R. Toor, *Parapositronium decay into three photons and implications for the neutral pion*, Phys. Rev. D **113**, 073002 (2026), [2602.14899](#).
- [25] E. W. N. Glover and A. G. Morgan, *Z boson decay into photons*, Z. Phys. **C60**, 175–180 (1993).
- [26] A. Denner and S. Dittmaier, *Electroweak Radiative Corrections for Collider Physics*, Phys. Rept. **864**, 1–163 (2020), [1912.06823](#).